

Numerical Simulation of Vortex Shedding from Bluff-Body Stabilised Flame with Cross Injection

Sombuddha Bagchi¹, Sourav Sarkar², Uddalok Sen³,
Achintya Mukhopadhyay⁴ and Swarnendu Sen⁵

^{1,2,4,5}Dept. of Mechanical Engg., Jadavpur University

³Dept. of Mechanical Engg., University of Illinois, Chicago

E-mail: ¹sombuddha.bagchi@gmail.com, ²souravsarkar.iitm@gmail.com, ³uddalok.sen.us@gmail.com,

⁴achintya.mukho@gmail.com, ⁵sen.swarnendu@gmail.com

Abstract—A laminar, two-dimensional transient flow past a cylindrical bluff body with cross-flow arrangement is investigated. The unstructured grid finite volume method is used and simulations were carried out using a commercial CFD package ANSYS 14.5. The injection velocity of methane is kept equal to three times the free stream velocity. First, the cold flow behavior is observed for two cases; without dilution and dilution with N_2 . Then, it is compared to the hot flow for the same cases: a rich flame and a lean diluted flame with N_2 . From the Fast Fourier Transform plots, the cold flow is observed to oscillate at various discordant frequencies and substantial noise is observed. However, for the hot flow, one dominant frequency is obtained. The flame is anchored right in front of the cylinder and persists for the lean combustion. The amplitude of vortex shedding for lean combustion is observed to increase by almost a factor of 20.

1. INTRODUCTION

Nowadays, NO_x emission control has become a principal source of concern of aerospace and automobile industries due to the stringency of emission control rules and regulations. Lean combustion is preferred over rich combustion to reduce NO_x emission because high temperature combustion with rich flame is identified as the primary source of NO_x formation. However, lean combustion is susceptible to be instability and leads to large-amplitude oscillations, unacceptable noise and even structural damage of the combustion systems [1,2]. Hence, in practical combustors like ramjet and turbojet afterburner, bluff body flame stabilizer is installed. Mixing shear layer formed at the downstream of the bluff body supports the stabilization of the flame. However, the flow pattern in the wake behind is both intricate and fascinating, and it is identified as one of the classical problem of fluid mechanics as it has different interesting flow features. At certain values of Reynolds number, asymmetrical Von Karman vortex shedding pattern is one of the most interesting feature in flow past a cylinder situation. This shedding pattern is intensively studied as it is of crucial importance in bluff body stabilized combustors. Flow past a cylinder has been the focus of active research for a long time across the world.

Posdziech and Grundmann [3] used the spectral element method for the numerical calculation of fundamental quantities of the 2-D flow past a circular cylinder at Reynolds number between 5 and 250. Wang et al. [4] studied the POD analysis of a wall mounted finite-length cylinder near wake and found out the relation between the orientation of the vortex shedding and the coefficients of the POD mode. Norberg [5] studied the temporal variation of the lift coefficients for the unconfined flow past a circular cylinder for a large range of Reynolds numbers. Mondal et al. [6] experimentally studied a bluff body stabilized laboratory-scale pulse combustor to investigate the effects of different parameters on combustion instability. Griffith et al. [7] testified the incidence of a two-dimensional instability of the periodic vortex shedding past a circular cylinder placed between two parallel walls, which leads to beating phenomenon of the lift and drag coefficients. Uddalok et al. [8] studied the transient, 2-D laminar flow past a circular cylinder with injection of methane. Fujii et al. [9] has compared cold and reacting flows around a bluff-body flame stabilizer for homogeneous propane/air mixture.

Transient flow past a circular cylinder has been studied in our current work. The bluff body i.e. the cylinder has two slots perpendicular to the direction of the flow, both of them 180° apart. This arrangement is actually referred to as a cross-flow arrangement. Methane is injected through the two slots at a particular velocity. Here, a comparison of the flow has been done between two cases. First, the flow past a circular cylinder has been done without any ignition i.e. the cold flow is studied in detail. Second, the flow past the cylinder is studied after the ignition is done. For the hot flow i.e. after the combustion has taken place, the flow past a circular cylinder has been observed at rich combustion and lean combustion. Similarly, the cold flow i.e. in absence of combustion has been considered for two cases; no dilution and dilution with N_2 . The commercial CFD package ANSYS Fluent 14.5 has been used to carry out the aforementioned simulations at a free stream Reynolds number of 100. Post-processing of the

acquired data has been done using TecPlot 360 software. A Fast Fourier Transforms is done using MATLAB to determine the frequency of vortex shedding for both the cases.

2. PROBLEM GEOMETRY

A rectangular unconfined flow domain (200 mm x 200mm) is considered and the slotted cylinder is placed centrally within the flow domain. The maximum diameter of the cylinder is 6 mm and two diametrically opposite slots are placed perpendicular to the direction of the flow 180° apart. Schematic of geometry is presented in figure 1. The ratio of injection velocity to free stream velocity is denoted by ϵ while the mass fraction of methane is symbolized by ϕ . In this configuration, the direction of injection velocity of methane is along the positive and negative y-direction and has a value equal to three times the free stream velocity or $\epsilon=3$, for both the hot flow and the cold flow. The cold flow is diluted from $\phi=1$ to $\phi=0.5$ and the effect of this dilution has been studied. Similarly, the hot flow is investigated for both rich ($\phi=1$) and lean ($\phi=0.5$) combustion. The free stream Reynolds number of 100 is considered for the present study. A velocity inlet condition is specified at the inlet, pressure-outlet condition at the outlet and a specified shear of zero magnitude at the two walls.

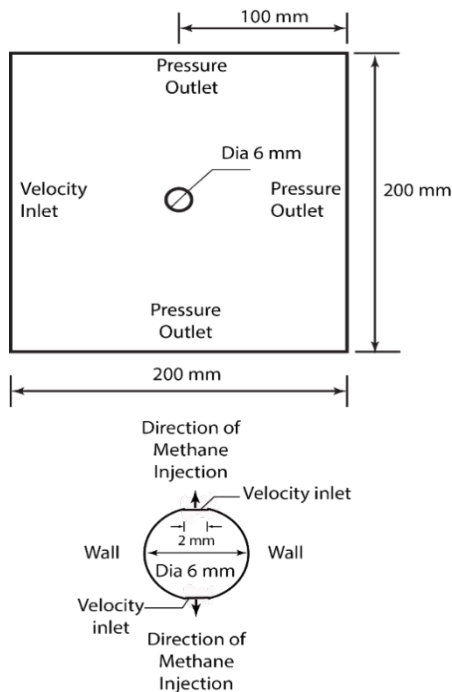


Fig. 1: Geometry and boundary conditions

3. GOVERNING EQUATIONS

For incompressible, laminar, 2-D transient flow the following governing equations has been used:

3.1 Continuity:

$$\frac{\partial \rho}{\partial t} + \nabla \cdot (\rho \vec{V}) = 0 \quad (1)$$

3.2 Momentum:

$$\frac{\partial (\rho \vec{V})}{\partial t} + \nabla \cdot (\rho \vec{V} \vec{V}) = -\nabla p + \nabla \cdot \vec{\tau} + \rho \vec{g} \quad (2)$$

where p is the static pressure, $\vec{\tau}$ is the stress tensor, $\rho \vec{g}$ is the gravitational body force and \vec{F} is any other external body force such as that arising from interaction with the discrete phase.

The stress tensor is given by

$$\vec{\tau} = \mu \left[(\nabla \vec{V} + \nabla \vec{V}^T) - \frac{2}{3} (\nabla \cdot \vec{V}) I \right]$$

3.3 Lift coefficient:

The lift coefficient is defined by the following relation

$$C_L = \frac{F_L}{\frac{1}{2} \rho U_\infty^2 D} \quad (3)$$

3.4 Strouhal number:

$$St = \frac{fD}{U_\infty} \quad (4)$$

3.5 Energy Equation:

$$\frac{\partial (\rho E)}{\partial t} + \nabla \cdot [\vec{V} (\rho E + p)] = \nabla \cdot [k \nabla T] - \sum_j h_j J_j + \nabla \cdot \tau V + Sh \quad (5)$$

The energy is given by

$$E = h - \frac{p}{\rho} + \frac{V^2}{2}$$

where

$$h = \sum_j Y_j h_j + \frac{p}{\rho}$$

$$h_j = \int_{T_{ref}}^T C_{p,j} dT$$

The reference temperature was taken to be 298.15 K.

3.6 Species Transport Equation:

$$\frac{\partial (\rho Y_i)}{\partial t} + \nabla \cdot (\rho \vec{V} Y_i) = -\nabla \cdot J_i + R_i + S_i \quad (6)$$

Where R_i is a reaction source term and S_i represents other source terms, which is generated from the discrete phase. For N species, generally $N - 1$ species equations are solved. The N^{th} species mass fraction is determined by subtracting from 1. Nitrogen is taken to be the N^{th} species.

J_i is the diffusion flux of species i

$$J_i = -\rho D_{i,m} \nabla Y_i - D_{T,i} \frac{\nabla T}{T} \quad (7)$$

The Laminar finite rate model was used to calculate source term R_i . As gas flows are laminar in this study, laminar finite rate model is chosen. For a reversible reaction, the molar rate of generation of a species i in reaction r is given by the expression

$$R_i = \Gamma(v_i'' - v_i') \left[k_{f,r} \prod_{j=1}^N C_{j,r}^{v_{j,r}'} - k_{b,r} \prod_{j=1}^N C_{j,r}^{v_{j,r}''} \right]$$

(8)

The rate constants are calculated as

$$k_{f,r} = A_r T^{\beta_r} e^{\frac{E_r}{RT}}$$

$$k_{b,r} = \frac{k_{f,r}}{K_r}$$

Where K_r is the equilibrium constant of the r^{th} reaction calculated from enthalpy and entropy of the species evaluated at the respective temperature and pressure. A reduced reaction mechanism with 16 species and 46 reactions was used to model chemistry of the combustion phenomena. All the other data for evaluation of the rate constants are provided through the thermodynamic and transport database files in FLUENT.

4. NUMERICAL METHODS AND VALIDATION

A finite volume based CFD code ANSYS Fluent 14.5 has been used to perform the required numerical simulations. The pressure based solver is chosen as the numerical scheme, and second order implicit transient solutions are performed. The laminar viscous model is used as the Reynolds number of the flow is 100. A least squares cell based scheme is employed for gradient calculations. SIMPLE scheme is used for pressure-velocity coupling and QUICK scheme was used for discretization of momentum equation. The convergence criteria for continuity and momentum equations were set at 10^{-3} .

The ANSYS Meshing package is used to create a triangle based unstructured grid. For better results and finer meshing around the central region, inflation is carried out with least element size of $10^{-7} m$ having 80 layers and a growth rate of 1.5. Grid independence study along with time independence is carried out to select the optimum mesh and time step for simulation. It is carried out by replacing the bluff body by a regular cylinder of the same diameter. The Reynolds number of the free stream is 100. Grid independence study was again carried out post combustion to validate the mesh.

This mesh and a time step size of 0.001 is considered to be optimum for simulation to reduce the computational time without any considerable loss in accuracy.

5. RESULTS AND DISCUSSION

The velocity contours for the hot and cold flow for $\epsilon=3$ and $\phi=1$ and 0.5 are compared and shown in the Fig. 2- Fig.5.

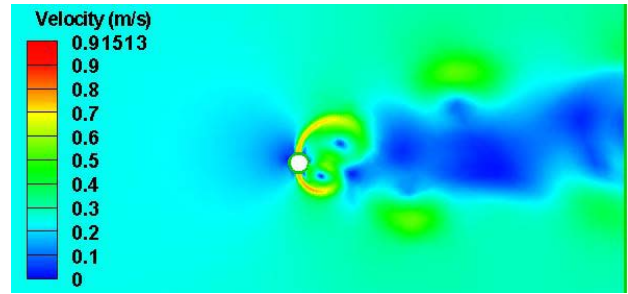


Fig. 2: Velocity contours of cold flow at $\phi=1$

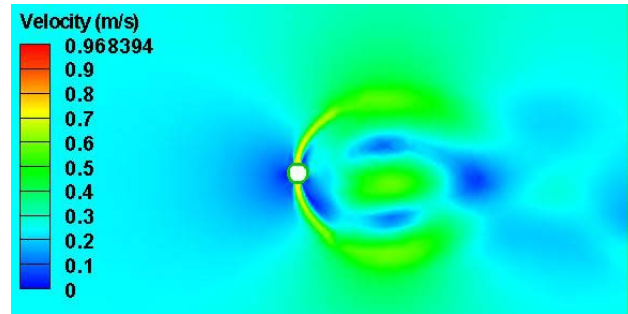


Fig. 3: Velocity contours of cold flow at $\phi=0.5$

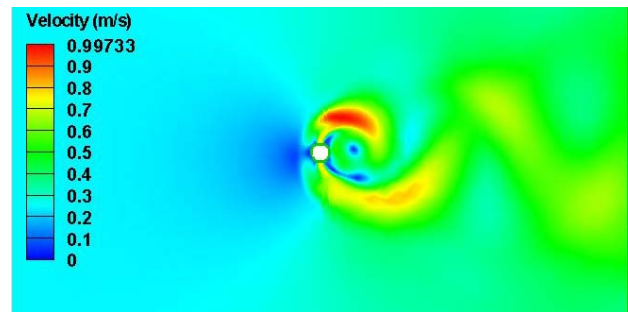


Fig. 4: Velocity contours of hot flow at $\phi=1$

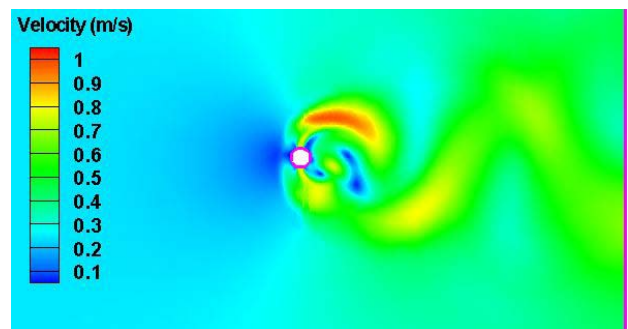


Fig. 5: Velocity contours of hot flow at $\phi=0.5$

The vorticity contours of hot and cold flow for $\phi=1$ and 0.5 are analyzed and presented in Fig. 6- Fig. 9.

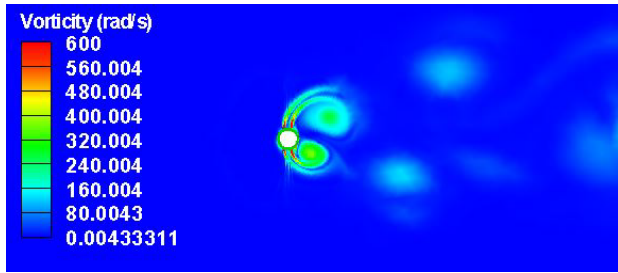


Fig. 6: Vorticity contours of cold flow at $\phi=1$

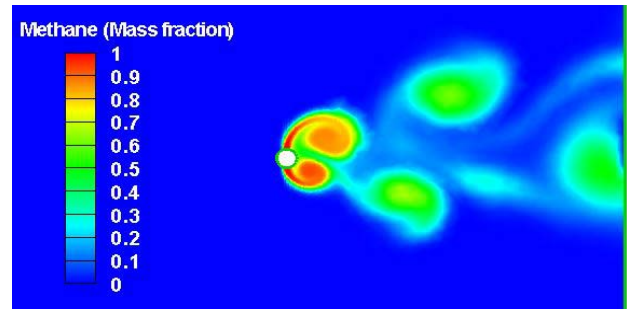


Fig. 10: Mass fraction of methane for cold flow at $\phi=1$

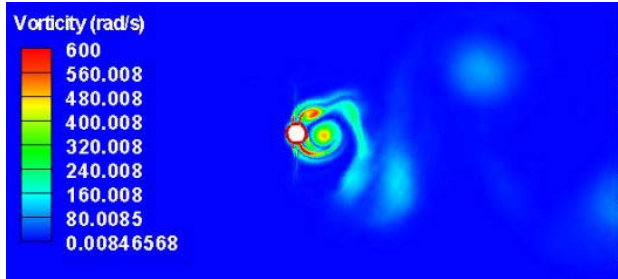


Fig. 7: Vorticity contours of cold flow at $\phi=0.5$

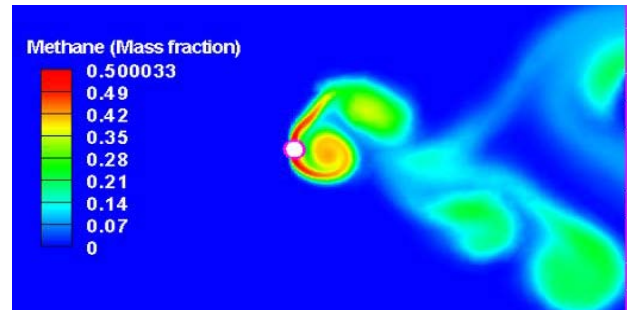


Fig. 11: Mass fraction of methane for cold flow at $\phi=0.5$

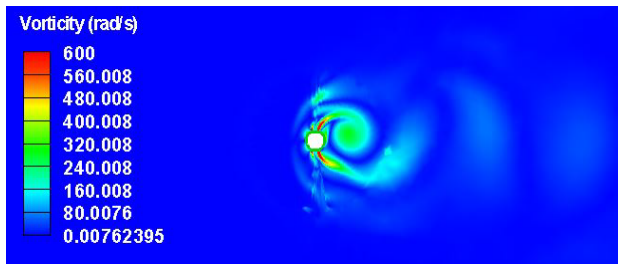


Fig. 8: Vorticity contours of hot flow at $\phi=1$

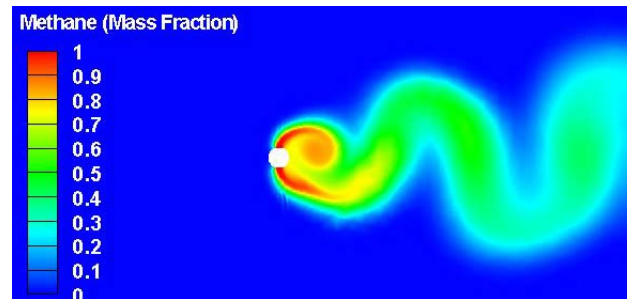


Fig. 12: Mass fraction of methane for hot flow at $\phi=1$

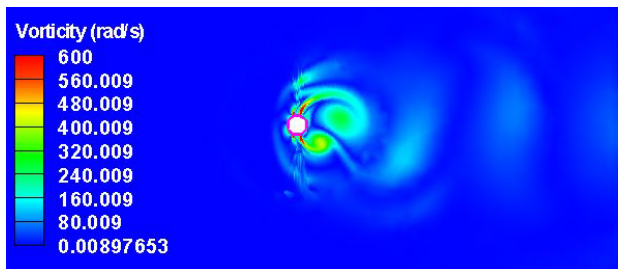


Fig. 9: Vorticity contours of hot flow at $\phi=0.5$

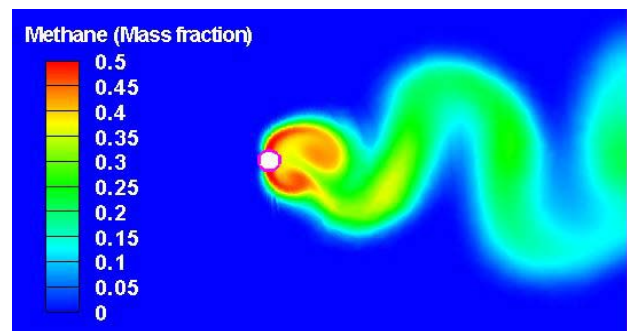


Fig. 13: Mass fraction of methane for hot flow at $\phi=0.5$

The mass fraction of methane contours of hot and cold flow for $\phi=1$ and 0.5 are illustrated in Fig. 10- Fig. 13.

The temperature and hydroxyl ion contours which is an indicator of where the actual combustion has taken place is shown in Fig 14 to Fig 17.

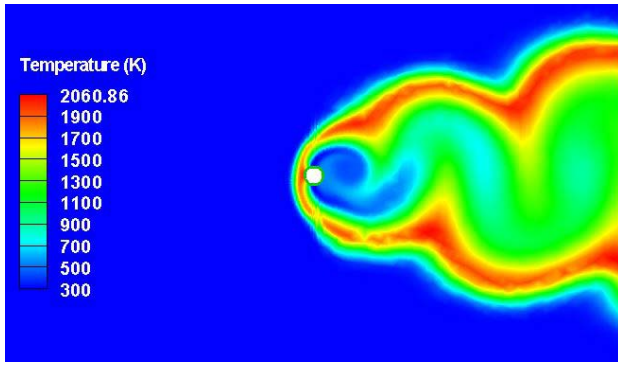


Fig. 14: Temperature contours of hot flow at $\phi=1$

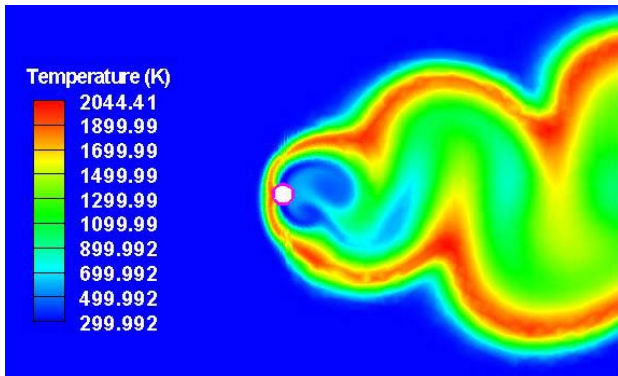


Fig. 15: Temperature contours of hot flow at $\phi=0.5$

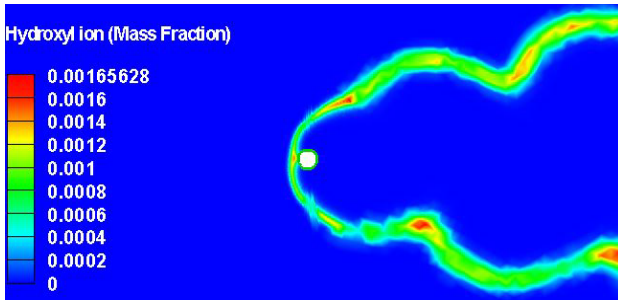


Fig. 16: Hydroxyl ion contours of hot flow at $\phi=1$

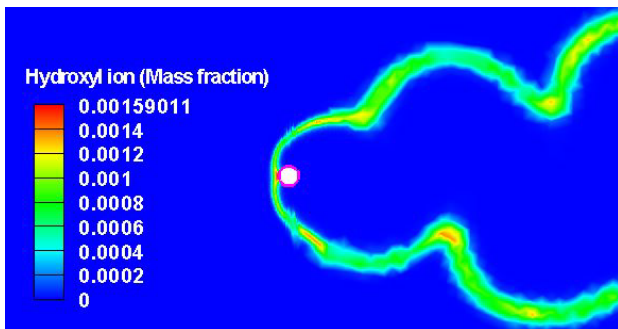


Fig. 17: Hydroxyl ion contours of hot flow at $\phi=0.5$

The lift coefficient of the flow is monitored and Fast Fourier Transform (FFT) is done on the results achieved. The corresponding FFT plots are shown as follows (Fig. 16-19). The visible peaks represent the dominant frequencies of vortex shedding. The Strouhal number is calculated from the corresponding frequencies in the FFT plots. For the hot flow at $\phi=1$, the frequency of vortex shedding was observed to be 7.830Hz ($St=0.193$) while the lean combustion, i.e. $\phi=0.5$ had a frequency of 7.328Hz ($St=0.180$). The FFT plots of cold flow exhibited more than one peaks of vortex shedding. The flow with diluted injection of methane had 4 dominant peaks of vortex shedding of frequencies 1.955Hz ($St=0.048$), 4.399Hz ($St=0.108$), 7.331Hz ($St=0.181$) and 9.775Hz ($St=0.241$) while the flow with no dilution of methane displayed 3 peaks at 4.888Hz ($St=0.120$), 6.354Hz ($St=0.157$) and 8.798Hz ($St=0.217$).

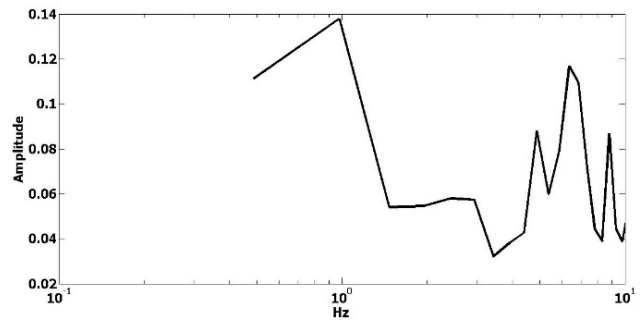


Fig. 18: FFT plot of cold flow at $\phi=1$

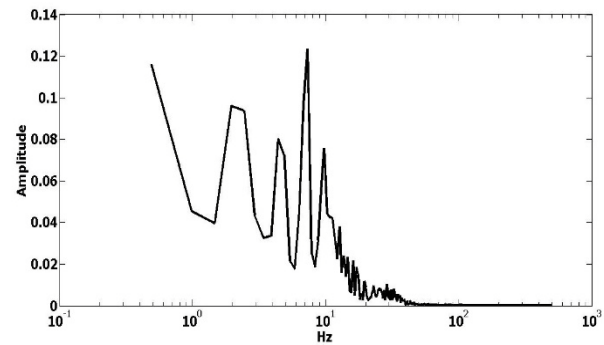


Fig. 19: FFT plot of cold flow at $\phi=0.5$

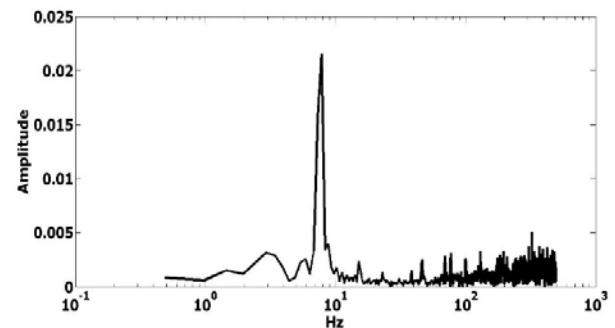


Fig. 20: FFT plot of hot flow at $\phi=1$

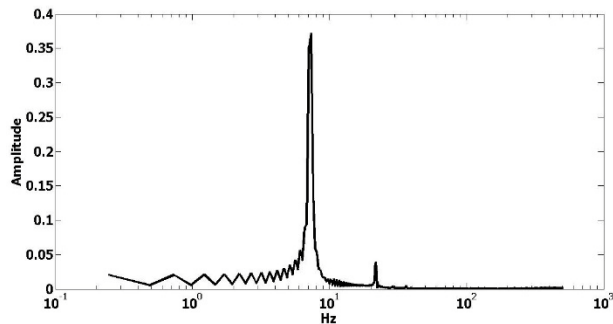


Fig. 21: FFT plot of hot flow at $\phi=0.5$

6. CONCLUSION

It can be concluded from the numerical investigations performed in the above experiment that the cold flow and the hot flow differ from each other both qualitatively and quantitatively with and without dilution, as is evident from the contours and FFT plots. Substantial amount of noise is observed in cold flow and the cylinder oscillates at more than one discordant frequencies. The amplitude of vortex shedding increases by almost a factor of 20 for cold flow. For the hot flow, the frequency of vortex shedding decreases by a small amount for lean combustion. The flame is anchored right in front of the cylinder and persists for both the cases. The flame is stable and continues to burn without losing heat. Hence, in order to reduce NO_x emissions, lean combustion can be performed successfully.

REFERENCES

- [1] Thevenin D., Renard P.H., Fiechtner G.J., Gord J.R., Rolon J.C., 2000. "Regimes of non-premixed flames vortex interactions". *Proc. Energy Combust. Sci.*, Vol. 26(3), 225–282.
- [2] Candel, S., 2002, "Combustion dynamics and control: Progress and challenges", *Proc. Combust. Inst.* Vol. 29, 1-28.
- [3] O. Posdziech, R. Grundmann. "A systematic approach to the numerical calculation of fundamental quantities of the two-dimensional flow over a circular cylinder", *J. Fluids Struct.*, Vol. 23 (2007), 479-499.
- [4] H. F. Wang, H. L. Cao, and Y. Zhou, "POD analysis of a finite-length cylinder near wake," *Exp. Fluids* 55, 1790 (2014), 1-15.
- [5] Norberg C., "Fluctuating lift on a circular cylinder: review and new measurements", *J. Fluids Struct.*, Vol. 17 (2003), 57-96.
- [6] Mondal S., Mukhopadhyay A., Sen S., "Dynamic Characterization of a Laboratory-Scale Pulse Combustor", *Combust. Sci. and Tech.*, Vol. 186.2 (2014), 139-152.
- [7] Griffith M. D., Leontini J., Thompson M.C., Hourigan K., "Vortex shedding and three-dimensional behavior of flow past cylinder confined in a channel", *J. Fluids Struct.*, Vol. 27 (2011), 855-860.
- [8] Sen U., Mukhopadhyay A., Sen S., 2017, "Effects of fluid injection on dynamics of flow past a circular cylinder", *Eur. J. Mech. B/Fluids.*, Vol. 61, 187-199.
- [9] Fujii S., Eguchi K., "A comparison of cold and reacting flows around a bluff-body flame stabilizer", *J. Fluids Eng.*, Vol. 103.2 (1981), 328-334.